P2X7 Receptor Antagonist Attenuates Retinal Inflammation and Neovascularization Induced by Oxidized Low Density Lipoprotein

Mingzhu Yang
Henan Provincial People's Hospital
Ruiqi Qiu
Henan Provincial People's Hospital
Weiping Wang
Henan Provincial People's Hospital
Jingyang Liu
Henan Provincial People's Hospital
Ya Li
Henan Provincial People's Hospital
Qing Zhu
Henan Provincial People's Hospital
Bo Lei (bolei99@126.com)
https://orcid.org/0000-0002-5497-0905

Research

Keywords: Retinal inflammation, Neovascularization, P2X7R antagonist, NLRP3 inflammasome, NF-kB signaling pathway

Posted Date: July 6th, 2020

DOI: https://doi.org/10.21203/rs.3.rs-39937/v1

Version of Record: A version of this preprint was published at Oxidative Medicine and Cellular Longevity on August 19th, 2021. See the published version at https://doi.org/10.1155/2021/5520644.

Abstract

Background: Inflammation and neovascularization are two vital pathological phases of AMD. Recent evidence indicates that blocking P2X7 receptor may relieve inflammation. Here, we investigated whether A740003, a P2X7 receptor antagonist, could prevent retinal inflammation and neovascularization induced by ox-LDL and explored the underlying mechanisms.

Methods: ARPE-19 cells were pretreated with A740003 for 2 hours before ox-LDL exposure. Western Blot, ELISA and qPCR were used to detect the proteins and mRNA levels of NLRP3, Caspase-1, P2X7R, pIKBa, IKBa, angiogenic factors and inflammatory cytokines. ROS assay was performed to detect the ROS generation. C57BL/6 mice were subretinally injected with ox-LDL to induce retinal inflammation and neovascularization. A740003 was administrated intraperitoneally starting from day 3 before to day 14 after ox-LDL injection. Retinal function was assessed by dark- and light-adapted ERG. Retinal neovascularization was detected by retinal whole flat mount and immunofluorescence. Thickness of INL and ONL was measured to evaluate the retinal edema.

Results: ox-LDL induced inflammatory responses and VEGF overproduction in human RPE cells and mouse retinas. However, A740003 decreased the expression of NLRP3, P2X7R, HIF-1a and VEGF in ARPE-19 cells. Inflammatory cytokines including IL-1b and IL-18 were down-regulated in A740003 treated cells. A740003 suppressed ROS generation and inhibited the phosphorylation of IKBa significantly. Whole flat mount of retinas and immunofluorescence showed that A740003 inhibited the angiogenesis induced by ox-LDL *in vivo*. The elevated mRNA and protein levels of NLRP3, Caspase-1, P2X7R, HIF-1a and VEGF decreased and IL-1b release was repressed in A740003 treated mice. Besides, the phosphorylation of IKBa was suppressed in the retinas of A740003 treated mice. The retinal edema was alleviated by A740003 treatment. The b- and a-wave amplitudes of ERG were remarkably preserved in A740003 treated mice.

Conclusions: A740003 significantly reduced ocular inflammatory responses and VEGF production in ARPE-19 cells. In addition, the P2X7R antagonist reduced retinal inflammation, neovascularization, and protected retinal function in mice. The protective effects were associated with regulating of NLRP3 inflammasome and NF-kB pathway, suppression of ROS generation, as well as inhibition of angiogenic factors.

Introduction

Age-related macular degeneration (AMD) is a blinding disease among people over age of 50 worldwide. The prevalence of AMD is expected to increase dramatically as the global population ages [1]. AMD is closely related with the chronic inflammation in retinal pigmented epithelial (RPE) cells, Bruch membrane and choroid membrane [2, 3]. There are two types of AMD according to the clinical characteristics, dry AMD and wet AMD. Dry AMD, also called non-exudative AMD, is characterized by retinal inflammation, which mainly happens in the early stage of AMD. Wet AMD, also called exudative AMD, is characterized

by choroidal neovascularization and retinal angiogenesis, which usually happens in the late stage of AMD [4]. Better understanding of the pathogenesis of AMD is crucial for seeking better and earlier treatment modalities.

The total cholesterol, triacylglycerol and low density lipoprotein (LDL) are obviously higher in AMD patients compared to normal people [5]. Moreover, LDL is susceptible to oxidation, resulting in the formation of ox-LDL [6]. ox-LDL can induce a large amount of reactive oxygen species (ROS) and oxidative stress injury. Chronic oxidative stress contributes to the pathogenesis of AMD. ox-LDL leads to lipid deposition, inflammation and pyroptosis when it is accumulated in cells. It is reported that high level of ox-LDL may lead oxidative stress and inflammation in glaucoma patients, which impedes wound healing after surgery [7]. The RPE becomes vulnerable to apoptosis through a number of mechanisms including the high oxidative stress environment. Oxidized low density lipoproteins (ox-LDL) are also internalized by the RPE, and alter photoreceptor turnover and lysosomal function [8]. The oxysterols in ox-LDL are cytotoxic to RPE cells [8, 9]. It is found that ox-LDL induces a pathologic response in RPE, which suggests that ox-LDL is one trigger for initiating early events in the pathogenesis of AMD [10].

Retinal angiogenesis may also relate with the overproduction of ox-LDL and ROS generation. Recently, it is reported that ox-LDL is immunohistochemically detected in surgically excised choroidal neovascular membranes from eyes with AMD [11]. ox-LDL levels were higher in peripheral blood of AMD patients with choroidal neovascularization compared to normal individuals [12], which suggested a close relationship between ox-LDL and AMD. ox-LDL may also induce retinopathy through damaging the blood capillary [13]. These researches suggest that ox-LDL may induce retinal inflammation and neovascularization.

Pyroptosis related with NLRP3 inflammasome activation is recently identified to be a novel type of programmed cell death. The canonical inflammasome complexes are assembled around protein members of the nod-like receptor (NLRs) and composed of apoptosis-associated speck-like protein containing a caspase recruitment domain (ASC), converting the pro-Caspase-1 zymogen into a catalytically active enzyme [14]. NLRP3 inflammasome senses and responds to a diversity of pathogens or danger-associated molecular patterns. Overproduction of ROS activates NLRP3, recruiting ASC and regulating auto-activation of pro-Caspase-1. After activation of pro-Caspase-1, pro-IL-1β and pro-IL-18 are cleaved into mature peptides and secreted outside to mediate the following inflammation [15]. Activation of NF-κB pathway upregulates the transcription of NLRP3 and pro-IL-1β. Ox-LDL induces a large amount of ROS in macrophage cells and activate NLRP3 inflammasome, and then promote the secretion of inflammatory cytokines such as IL-1b and IL-18 [16]. Beside, the ROS mediated by ox-LDL also leads the activation of NF-κB signaling pathway, which may strengthen the inflammation response [14].

The P2 × 7 receptor (P2 × 7R) is an ATP-gated ion channel which is a key player in oxidative stress under pathological conditions. P2 × 7R is expressed in the RPE and neural retina. Activation of P2 × 7R induces calcium ion influx and leads the interaction of P2 × 7R and NLRP3 inflammasome and thus activates the NLRP3 signaling pathway. It was reported that P2 × 7R played a critical role in regulating the normal

physiological functions of macrophages and monocytes and it may induce the synthesis and secretion of inflammatory cytokines [17].

P2 × 7R activation is always followed by the activation of NLRP3 inflammasome. A740003, an effective P2 × 7R antagonist, is commonly used in previous studies. Recently, it is reported that P2 × 7R antagonist protects retinal ganglion cells by inhibiting microglial activation [18]. Besides, blocking of the P2 × 7R inhibits the activation of NF-κB pathways in the cartilage tissue [19]. Therefore, we speculated that P2 × 7R inhibitor attenuated retinal inflammation induced by ox-LDL through regulating the activation of NF-κB pathway and NLRP3 inflammasome, and reduced retinal angiogenesis by downregulating the expression of VEGF and HIF-1α.

Materials And Methods

Preparation of ox-LDL and A740003

Human ox-LDL was purchased from Solarbio Science & Technology Co., Ltd (Beijing, China). ARPE-19 cells were exposed to 100 μg/ml ox-LDL diluted with DMEM/F12 medium. Concentration of 3.0 mg/ml ox-LDL was used for subretinal injection of C57BL/6 mice. A740003 (ApexBio, Huston, TX, USA) was dissolved in 100% dimethyl sulfoxide (DMSO) and diluted with DMEM/F12 medium or PBS to a final DMSO concentration no more than 1%. DMEM/F12 dilution was used for ARPE-19 treatment and PBS dilution was used for intraperitoneal injection of C57BL/6 mice.

Cell Culture And Treatment

ARPE-19 cells were purchased from the American Type Culture Collection (ATCC, Manassas, VA, USA). ARPE-19 cells were grown in DMEM/F12 medium (Gibco, New York, NY, USA) supplemented with 10% FBS (TBD science, Tianjin, China), 1% penicillin and streptomycin (Solarbio) in 37 °C with 5% CO2 incubator. The optimal ox-LDL concentration for following studies was 100 μg/ml, which was chosen based on the mRNA expression levels of NLRP3 and VEGF. The optimal concentration is corresponding to the previous report [20]. After 24 hours starvation, ARPE-19 cells were exposed to 100 μg/ml of ox-LDL for 24 hours with 2 hours pretreatment of 1 μM A740003. Besides, ARPE-19 cells were pretreated with 200 μM of A740003 for 2 hours, followed by stimulation of 100 μg/ml ox-LDL for 48 hours. The optimal concentrations of A740003 for 24/48 hours exposure to ox-LDL were screened by quantitative real-time PCR results.

Animal Care And Use

Male C57BL/6 mice were purchased from Jackson Laboratories (Bar Harbor, ME, USA). The animals were housed under 12-h light-dark cycle and given a standard chow diet. Animal care followed the guidelines formulated by the Association for Research in Vision and Ophthalmology (ARVO). Experiments and

procedures involving animals were permitted by the Ethics Committee of Henan Eye Institute. Every effort was made to minimize animal discomfort and stress.

Mice of 6 ~ 8-week-old were randomly divided into four groups: (1) Control group: treated with subretinal injection of 1 μL PBS (Solarbio); (2) ox-LDL group: treated with subretinal injection of 1 μL ox-LDL (3.0 mg/ml) (Sigma-Aldrich, St. Louis., MO, USA); (3) ox-LDL + Vehicle group: treated with subretinal injection of 1 μL ox-LDL (3.0 mg/ml). 1% DMSO with PBS served as vehicle and was intraperitoneally injected daily from day 3 before to day 14 after ox-LDL subretinal injection; (4) ox-LDL + A740003 group: treated with subretinal injection of 1 μL ox-LDL (3.0 mg/ml). A740003 (30 mg/kg/d) was intraperitoneally injected daily from day 3 before to day 14 after ox-LDL injection. Two weeks after subretinal injection of ox-LDL, mice were sacrificed for following experiments.

Subretinal Injection Of Ox-ldl

One μL ox-LDL (3.0 mg/ml) was injected subretinally into the right eyes of the mice, and the lateral eyes were not injected. Injection was performed according to a protocol described previously [21]. Briefly, mice were anesthetized with intraperitoneal injection of 4% chloral hydrate (10 ml/kg). Pupils were dilated with tropicamide phenylephrine eye drops (Santen Pharmaceutical Co., Ltd, Osaka, Japan) 10 minutes prior to injection. An aperture within the dilated pupil area was made through the sclera, below the ora serrata with a 30-gauge needle. Then a blunt 32-gauge Hamilton syringe was inserted through the aperture, avoiding damage of the lens and penetrating the neuroretina. One μL ox-LDL was injected into subretinal space under the dissecting microscope. Successful delivery of ox-LDL was confirmed by viewing subretinal blebs demarcating the retinal detachment in the injected retinal area. Such detachments usually resolved within 1 to 2 days. All animals received antibiotic eyedrops to the cornea and were observed daily after operation. Only animals with minimal surgical complications and initial retinal blebs occupying more than 60% the retina were retained for further study.

Real-time Quantitative Pcr Analysis

ARPE-19 cells were collected by digestion of 0.25% trypsin and centrifuging. Eyeballs of mice were enucleated at 2 weeks after ox-LDL subretinal injection. Retinas were dissected and homogenized for total RNA extraction. The mRNA levels of NLRP3, Caspase-1, P2 × 7R, VEGF, HIF-1α in ARPE-19 cells and retinas were detected by qPCR assay. Total RNA was extracted with Trizol reagent (ThermoFisher Scientific, Waltham, MA, USA) from ARPE-19 cells and retinas according to the manufacturer's instructions. Complementary DNA (cDNA) was generated by using the PrimeScript® RT reagent kit (Takara Biotechnology, Dalian, China). qPCR was performed according to the manufacturer's instructions with the ABI Prism 7500 system (Applied Biosystems, Foster City, CA, USA). The amplification system used for qPCR was a volume of 20 μL PowerUp™ SYBR® Green Master Mix (ThermoFisher Scientific). The cycling protocol comprised of 50 °C for 2 minutes, and then 95 °C for 2 minutes, followed by 40 cycles at 95 °C for 15 seconds and 60 °C for 1 minute. To determine the mRNA expression, which was

normalized to the endogenous reference gene β-actin, all samples were detected in triple. Relative quantification was achieved by the comparative $2^{-\Delta\Delta Ct}$ method. The sequences of primers used for qPCR assay are shown in Table 1 and Table 2.

Table 1
Sequences of Primers for Human

Gene	Forward Primer	Reverse Primer
NLRP3	GATCGTGAGAAAACCCTCCA	GGTCCTATGTGCTCGTCAAA
P2 × 7R	AGGAAGAAGTGCGAGTCCATTGTG	CTGAACAGCTCTGAGGTGGTGATG
VEGF	CAGATTATGCGGATCAAACCT	ACGTTCGTTTAACTCAAGCT
HIF-1α	GAACGTCGAAAAGAAAAGTCTCG	CCTTATCAAGATGCGAACTCACA
β-actin	GCCAACCGCGAGAAGATGACC	CTCCTTAATGTCACGCACGATTTC

Table 2
Sequences of Primers for Mouse

Gene	Forward Primer	Reverse Primer
NLRP3	CTCTGTTCACTGGCTGCGGATG	TAGGACCTTCACGTCTCGGTTCAG
P2 × 7R	GCATAGCAGAGGTGACGGAGAATG	AGTAGGACACCAGGCAGAGACTTC
VEGF	CGAAGCTACTGCCGTCCGATTG	CCGCTCTGAACAAGGCTCACAG
HIF-1α	ACCTTCATCGGAAACTCCAAAG	CTGTTAGGCTGGGAAAAGTTAGG
Caspase-1	CGTGGAGAGAAACAAGGAGTG	AATGAAAAGTGAGCCCCTGAC
β-actin	TCACTATTGGCAACGAGCGGTTC	CTCCTGCTTGCTGATCCACATCTG

Enzyme-linked Immunosorbent Assay

After pretreatment with 100 μg/ml A740003 for 2 hours, ARPE-19 cells were induced with ox-LDL for 24 hours. Then supernatants of all groups were collected and centrifuged to detect the concentrations of IL-1β (Raybiotech, Norcross, GA, USA) and IL-18 (R&D Systems, Minneapolis, CA, USA) by using human ELISA kits according to the manufacturers' protocols. The concentrations of IL-1β and IL-18 were calculated according to optical density measured at 450 nm by subtracting the optical density measured at 540 or 570 nm using a multifunction microplate reader (PerkinElmer, Waltham, MA, USA).

Reactive Oxygen Species (ros) Assay

ARPE-19 cells were divided into four groups: (1) Control group: incubated with DMEM/F12 basal medium; (2) ox-LDL group: exposed to 100 μg/ml ox-LDL; (3) ox-LDL + Vehicle group: pretreated with DMSO for 2

hours and then exposed to 100 μg/ml ox-LDL; (4) ox-LDL + A740003 group: pretreated with A740003 for 2 hours and then exposed to 100 μg/ml ox-LDL. 24 hours later after exposure to ox-LDL, ARPE-19 cells were subjected to ROS assay according to manufacture's instruction (Beyotime, Shanghai, China). Briefly, ARPE-19 cells were exposed to 10 μM DCFH-DA probe for 30 minutes at 37 ℃ and then washed with DMEM/F12 basal medium for 3 times. Fluorescence of DCF was detected by fluorescent microscope at 488 nm excitation wavelength and 525 nm emission wavelength. The average optical density of each group was measured using Image-Pro Plus 6.0 software (Media Cybernetics, Inc., Rockville, MD, USA).

Western Blot Analysis

Cells were washed with PBS (Solarbio) for three times and lysed with lysis buffer for WB/IP assays (Yesen, Shanghai, China) containing 1% protease inhibitor cocktail (ApexBio, Houston, TX, USA) on the ice for 30 minutes. Similarly, retinas were dissected from eyeballs of mice and homogenized with lysis buffer containing 1% protease inhibitor cocktail on the ice for 30 minutes. The supernatants were collected after centrifuging the cell lysate at 12,000 rpm for 15 minutes. The protein concentration was detected by using bicinchoninic acid (BCA) protein kit (Beyotime). All samples were diluted with 5 × SDS loading buffer (EpiZyme, Shanghai, China) and boiled at 100 °C for 5 minutes. Equal amounts of total protein (80–100 μg) were separated on a 10% SDS-polyacrylamide gel and transferred to polyvinylidenedifluoride (PVDF) membranes (Millipore Corporation, Burlington, MA, USA). After blocking with 5% non-fat milk for 1.5 hours, the membranes were incubated with specific primary antibodies against NLRP3 (1:100, Cell Signaling Technology, Danvers, MA, USA), Caspase-1 (1:200, Abcam, Cambridge, MA, USA), P2 × 7R (1:1000, Novus Biologicals, Littleton, CO, USA), VEGF(1:450, Abcam), HIF-1α (1:1000, Novus), p-IκB-α (1:500, Abcam), IκB-α (1:1000, Abcam), IL-1β (1:500, Abcam) and β-actin (1:1000, Abcam) overnight at 4 °C. After washing, the membranes were incubated with secondary antibody (1:10000, Millipore) at room temperature for 2 hours under 50 rpm gently shaking. Signals were developed with ECL kit (Millipore), and band densitometry was performed using the AlphaView SA Software (ProteinSimple, San Jose, CA, USA). β-actin was used as loading control. Measurements were repeated three times for each experiment.

Electroretinogram (erg)

Retinal function was assessed with ERG following a previously described procedure [22]. After overnight dark adaptation, mice were anesthetized with intraperitoneal injection of 4% chloral hydrate (10 ml/kg). The pupils were dilated with tropicamide eye drops 30 minutes prior to recording. Needle electrodes were subcutaneously inserted into the back and the tail as reference and ground leads respectively. Active electrodes were gently positioned on the center of cornea. All procedures were performed under dim red light. Full-field ERGs were recorded with RetiMINER-C, a visual electrophysiology system (AiErXi Medical Equipment Co., Ltd., Chongqing, China). A series of stimulus intensities ranged from − 3 to 1 log cd-s/m^2 was applied for dark-adapted ERGs. After light adaptation of 5 minutes, light-adapted ERGs were

recorded to strobe-flash stimuli (0 and 1 log cd-s/m^2) superimposed on the background light. Responses to brief flashes were analyzed by measuring the amplitudes of the a- and b-waves.

Whole Flat Mount Of Mouse Retinas

Retinal whole flat mounts were prepared as previously described [23]. Briefly, the eyeballs from C57BL/6 mice were removed and fixed in 4% paraformaldehyde at room temperature for 1 hour. The cornea was cut an incision under dissecting microscope. At incision, the sclera was peeled towards optic nerve and then the lens and iris were removed. The retinas were extracted and permeabalized in 0.5%Tritonx-100 for 2 hours. The retinas were stained by isolectin-B4 for 30 minutes by gently shaking. After staining, the retinas were cut at 3, 6, 9, 12 o'clock for 4 incisions. Anti-fluorescence mounting media was used for resistance to fluorescence quenching before covering the retinas by coverslip. Flat-mounts were examined by fluorescence microscopy (Olympus, Tokyo, Japan).

Immunofluorescent Staining

Immunohistochemistry was performed using methodology as previously described [22]. Eyes were enucleated at 2 weeks after suretinal injection of ox-LDL and fixed with 4% paraformaldehyde overnight. After dehydration, the eyes were embedded in melting paraffin. Serial 4 μm paraffin sections were cut through cornea-optic nerve axis. Tissue sections were subsequently treated for antigen retrieval and blocked with 5% BSA for 30 minutes. Then sections were incubated with anti-VEGF antibody (1:200; Servicebio, Wuhan, China) overnight at 4℃. After washing, the slides were incubated with anti-rabbit secondary antibody for 50 minutes and DAPI for 10 minutes in dark. Anti-fluorescence mounting media was used for resistance to fluorescence quenching. Paraffin sections were examined under fluorescence microscope. The average optical density of each section was measured using Image-Pro Plus 6.0 software. The thicknesses of inner nuclear layer (INL) and outer nuclear layer (ONL) in each retina were measured and summarized.

Statistical analysis

Results from experiment were expressed as mean ± standard error of mean (SEM). Statistical analysis was analyzed by the GraphPad Prism 7 software (GraphPad Software, San Diego, CA, USA). Experimental data were analyzed by one-way ANOVA or two-way ANOVA followed by Bonferroni correction. *P* value less than 0.05 was considered as statistically significant.

Results

A740003 inhibited the activation of NLRP3 inflammasome, phosphorylation of IKBα and decreased the expression of P2 × 7R in ARPE-19 cells

ARPE-19 cells were cultured with 100 μg/ml of ox-LDL for 24 hours. Secretion of inflammatory cytokines was determined by ELISA. ELISA results showed that ox-LDL promoted the secretion of IL-1β (Fig. 1a) and IL-18 (Fig. 1b) significantly compared to control group. The up-regulated secretion of IL-1β and IL-18 indicated that more pro-IL-1β and pro-IL-18 were cleaved to mature inflammatory cytokines under the effects of mature Caspase-1. Pro-Caspase-1 turned into mature Caspase-1 when NLRP3 inflammasome was activated. Therefore, the ELISA results confirmed the activation of NLRP3 inflammasome in ARPE-19 cells exposed to ox-LDL. It indicated that ox-LDL induced the activation of NLRP3 inflammasome. Moreover, the qPCR assay was performed to determine the mRNA levels of NLRP3 and P2 × 7R. ox-LDL up-regulated the mRNA levels of NLRP3, P2 × 7R significantly (Fig. 1c, 1d). Western Blot was performed to evaluate the levels of proteins related with NLRP3 inflammasome. The results showed that the protein levels of NLRP3 (Fig. 1e, 1f), Caspase-1 (Fig. 1e, 1 g), P2 × 7R (Fig. 1e, 1h) and the phosphorylation of IKBα (Fig. 1e, 1i) in ARPE-19 cells increased obviously after exposure to ox-LDL.

Furthermore, ARPE-19 cells were pretreated with 1 μM A740003 for 2 hours before 24 hours ox-LDL incubation. ELISA results showed that A740003 pretreatment reversed the effects of ox-LDL incubation. It decreased the secretion of inflammatory cytokines including IL-1β (Fig. 1a) and IL-18 (Fig. 1b) significantly compared to vehicle-treated group. In addition, compared to vehicle-treated group, A740003 pretreatment decreased the mRNA levels of NLRP3 (Fig. 1c) and P2 × 7R (Fig. 1d) distinctly in ARPE-19 cells. A740003 inhibited the over expression of P2 × 7R and NLRP3 which were induced by ox-LDL. The Western Blot results showed that protein levels of NLRP3, Caspase-1, P2 × 7R increased robustly in ARPE-19 cells exposed to ox-LDL. However, pretreatment with A740003 could remarkably down-regulated the protein expression of NLRP3, Caspase-1 and P2 × 7R in ARPE-19 cells (Fig. 1e, 1f, 1 g, 1 h). The phosphorylation of IKBα was closely related with the activation of NF-κB signaling pathway. Western Blot results also showed that ox-LDL enhanced the ratio of p-IKBα to IKBα protein significantly. Moreover, the phosphorylation of IKBα was inhibited significantly in ARPE-19 cells pretreated with A740003 (Fig. 1e, 1i). In conclusion, the results suggested that the ox-LDL stimulation could up-regulate the secretion of inflammatory cytokines, which indicated the activation of NLRP3 inflammasome and pro-Caspase-1. However, P2 × 7R antagonist could inhibit the expression and secretion of inflammatory cytokines induced by ox-LDL. Moreover, the activation of of NLRP3 inflammasome and NF-κB signaling pathway induced by ox-LDL could be suppressed by A740003 treatment.

A740003 suppressed the up-regulation of angiogenic growth factors in ARPE-19 cells exposed to ox-LDL

ARPE-19 cells were treated with 100 μg/ml of ox-LDL for 48 hours. The qPCR assay was performed to determine the mRNA levels of VEGF and HIF-1α. The resutls were shown in Fig. 2, mRNA levels of VEGF and HIF-1α increased significantly in ARPE-19 cells exposed to ox-LDL (Fig. 2a, 2b). VEGF and HIF-1α are primary angiogenic proteins contributing to neovascularization. Thus the protein levels of VEGF and HIF-1α are vital for evaluating the possibility of retinal neovascularization. Western Blot was performed to detect the levels of proteins related with angiogenesis. The results demonstrated that the protein levels of VEGF and HIF-1α up-regulated obviously in ARPE-19 cells incubated with ox-LDL (Fig. 2c, 2d, 2e).

In addition, another group of ARPE-19 cells was pretreated with 200 μM A740003 for 2 hours before ox-LDL incubation. The qPCR and Western Blot assay were performed to determine the mRNA and protein levels of HIF-1α and VEGF in ARPE-19 cells pretreated with A740003. The results manifested that mRNA levels of VEGF and HIF-1α decreased evidently in ARPE-19 cells pretreated with A740003 (Fig. 2a, 2b). Furthermore, the protein levels of VEGF and HIF-1α were suppressed effectively by A740003 pretreatment in ARPE-19 cells (Fig. 2c, 2d, 2e). The results indicated that ox-LDL increased the mRNA and protein levles of angiogenic growth factors including VEGF and HIF-1α in ARPE-19 cells. Whereas, A740003 pretreatment could inhibited the HIF1α/VEGF axis effectively in ARPE-19 cells exposed to ox-LDL. A740003 might be effective to suppress the retinal neovascularization through inhibiting the HIF1α/VEGF axis.

A740003 suppressed the ROS generation induced by ox-LDL in ARPE-19 cells

ROS generation in ARPE-19 cells was detected by DCFH-DA fluorescent probe and microscope after 24 hours exposure to ox-LDL. The results showed that DCFH-DA fluorescent intensity was significantly increased after ox-LDL incubation compared to control group (Fig. 3a). Image-Pro Plus 6.0 software was used to calculate the average optical density (AOD) of each group. The results showed that average optical density in ox-LDL incubated group was obviously higher than control group (Fig. 3b). It indicated that ROS generation was successfully induced by ox-LDL incubation in ARPE-19 cells. Over production of ROS could activate the NLRP3 inflammasome and result in inflammation. Moreover, compared to vehicle-treated group, DCFH-DA fluorescent density in A740003 treated group was significantly decreased, suggesting that ROS production was effectively suppressed by A740003 pretreatment (Fig. 3a, 3b).

A740003 inhibited the activation of NLRP3 inflammasome, phosphorylation of IKBα and decreased the over expression of P2 × 7R in vivo

C57BL/6 mice were subretinally injected with 1 μL ox-LDL. A740003 (30 mg/kg/d) was intraperitoneally injected daily from 3 days before ox-LDL injection. Two weeks later, qPCR and Western Blot assay were performed to determine the mRNA and protein levels of NLRP3, P2 × 7R and Caspase-1. The protein level of IL-1β and phosphorylation of IKBα were also assessed by Western Blot. As shown in Fig. 4, mRNA levels of NLRP3, Caspase-1 and P2 × 7R were up-regulated significantly in mice injected with ox-LDL, whereas treatment with A740003 daily could inhibit the increase of NLRP3, Caspase-1 and P2 × 7R at mRNA level effectively compared to vehicle-treated group (Fig. 4a, 4b, 4c). Furthermore, Western Blot results demonstrated that protein levels of NLRP3, Caspase-1, IL-1β and P2 × 7R increased remarkably in mouse retinas injected with ox-LDL (Fig. 4d, 4e, 4f, 4 g, 4 h). It indicated that ox-LDL injection activated NLRP3 inflammasome. However, compared to vehicle-treated group, the protein levels of NLRP3, Caspase-1, IL-1β and P2 × 7R in mouse retinas of A740003 treated group decreased obviously (Fig. 4d, 4e, 4f, 4 g, 4 h). Subretinal injection of ox-LDL could increase the phosphorylation of IKBα and thus induce the activation of NF-κB signaling pathway (Fig. 4d, 4i). The Western Blot results also showed the ratio of p-IKBα to IKBα in mouse retinas of A740003 treated group significantly decreased compared to vehicle-treated group (Fig. 4d, 4i). The results showed that ox-LDL could activate the NLRP3 inflammasome and

NF-κB signaling pathway significantly. It indicated that A740003 treatment decreased the expression of P2 × 7R and suppressed the activation of NLRP3 inflammasome and NF-κB signaling pathway *in vivo*.

A740003 suppressed the expression of HIF-1α and VEGF in mice subretinally injected with ox-LDL

As previously described, C57BL/6 mice were subretinally injected with 1 μL ox-LDL. A740003 (30 mg/kg/d) was intraperitoneally injected daily from 3 days before ox-LDL injection. Two weeks later, qPCR and Western Blot assay were performed to determine the mRNA and protein levels of VEGF and HIF-1α. As shown in Fig. 5, mRNA levels of VEGF and HIF-1α were up-regulated significantly in mice subretinally injected with ox-LDL (Fig. 5a, 5b). Western Blot results manifested that protein levels of HIF-1α and VEGF increased remarkably in mice subretinally injected with ox-LDL (Fig. 5c, 5d, 5e). It indicated that ox-LDL subretinal injection up-regulated the angiogenic factors including VEGF and HIF-1α intensively, which would contribute to the retinal angiogenesis. In addition, Western Blot results showed that protein levels of VEGF and HIF-1α decreased remarkably in mice treated with A740003 daily (Fig. 5c, 5d, 5e). Therefore, the results confirmed that the retinal angiogenic factors induced by ox-LDL were suppressed by A740003 treatment.

A740003 prevented the retinal function impairment induced by ox-LDL in vivo

C57BL/6 mice were pretreated with A740003 daily from 3 days before ox-LDL injection. Two weeks after subretinal injection of ox-LDL, ERG was performed to evaluate the retinal function of mice injected with ox-LDL or PBS. Dark- and light-adapted ERGs showed that the amplitudes of a-wave and b-wave, which represented the functions of the photoreceptors and bipolar cells respectively, decreased significantly in mice subretinally injected with ox-LDL (Fig. 6a). However, the amplitudes of Dark-adapted a-wave and b-wave in A740003 treated mouse retinas were higher than vehicle-treated mice (Fig. 6b, 6c). The amplitude of light-adapted b-wave was also preserved by A740003 treatment (Fig. 6d). It indicated that A740003 treatment could alleviate retinal function impairment induced by ox-LDL in mice.

A740003 inhibited retinal angiogenesis by down regulating VEGF expression and reduced the retinal edema induced by ox-LDL in vivo

C57BL/6 mice were subretinally injected with ox-LDL and treated with A740003 daily from 3 days before ox-LDL injection. Two weeks later, immunofluorescent assay and retinal whole flat mount were processed to investigate the retinal angiogenesis and retinal edema in C57BL/6 mice. The results of immunofluorescent assay showed that ox-LDL increased the VEGF level robustly in retinas after two weeks of ox-LDL subretinal injection (Fig. 7a, 7b). However, A740003 decreased the VEGF expression induced by ox-LDL significantly in mice compared to vehicle-treated group (Fig. 7a, 7b). Besides, the immunofluorescent results also showed that thickness of INL and ONL increased significantly in ox-LDL group (Fig. 7a, 7c). It indicated that ox-LDL resulted in the retinal edema in mice. Compared to vehicle-treated group, the thickness of INL and ONL decreased obviously in A740003 treated group (Fig. 7a, 7c). The results suggested that A740003 inhibited the retinal edema induced by ox-LDL. The retinal whole flat mount showed that ox-LDL successfully induced the retinal angiogenesis in mice (Fig. **S1a**, **S1b**).

However, A740003 decreased the number of new blood vessels in retinas significantly compared to vehicle-treated group (Fig. **S1a**, **S1b**). The results indicated that A740003 suppressed the retinal angiogenesis and retinal edema induced by ox-LDL successfully.

Discussion

Accumulating evidence indicates that chronic inflammation in response to ox-LDL is implicated in the pathogenesis of AMD [10, 12, 20, 24]. In this study, we investigated the effects of ox-LDL on pro-inflammatory responses and pro-angiogenesis in human ARPE-19 cells and in a novel mouse model presenting inflammatory responses and neovascularization. We found A740003, a P2 × 7 receptor antagonist, significantly inhibited ox-LDL induced retinal inflammatory responses, neovascularization, ROS generation and alleviated retinal function impairment in ox-LDL treated cells and injected mice.

ox-LDL induced pro-inflammatory responses and pro-angiogenesis factors both in vitro **and** in vivo

The results showed that ox-LDL promoted the secretion of IL-1β, IL-18, HIF-1α and VEGF in ARPE-19 cells, indicating ox-LDL induced pro-inflammatory responses and pro-angiogenesis. Besides, we further investigated the diverse effects of ox-LDL on retinal inflammation and angiogenesis in ARPE-19 cells. Interestingly, we found 24 hours incubation with ox-LDL could promote the inflammatory cytokines significantly in ARPE-19 cells, while the expression of HIF-1α and VEGF showed no significance. However, 48 hours incubation with ox-LDL could promote the expression of HIF-1α and VEGF in ARPE-19 cells significantly. It suggested that pro-angiogenesis occurred after the inflammatory responses, which mimicked the development of AMD where inflammation usually precedes neovascularization. In addition, ox-LDL also induced production of ROS, which is involved in the process of AMD.

To confirm the role of ox-LDL in retina, we created a mouse model by subretinal injection of ox-LDL. Similar to those observed *in vitro*, we found IL-1β, HIF-1α and VEGF levels were significantly increased in the mouse retinas 14 days after subretinal injection. Furthermore, retinal function was compromised and neovascularization was evident in ox-LDL injected eyes. Since ox-LDL is a trigger for initiating early events in AMD, and since the major pathologic processes including inflammatory responses and neovascularization were seen in the novel model, we suggested it might be an appropriate one for studying AMD.

Blocking of P2 × 7R reduced pro-inflammatory responses and pro-angiogenesis factors both in vitro **and** in vivo

To test whether P2 × 7R is involved in the pathogenesis of AMD and to test whether blocking P2 × 7R would prevent the pro-inflammatory responses and pro-angiogenesis induced by ox-LDL, A740003, a P2 × 7R antagonist was applied to block P2 × 7R in human RPE cells and mouse model. The results demonstrated that A740003 decreased the secretion of inflammatory cytokines including IL-1b and IL-18 obviously both *in vitro* and *in vivo*. Moreover, the protein levels of VEGF and HIF-1a in A740003 treated group down-regulated evidently compared to vehicle-treated group both in cells and mouse retinas.

Retinal immunoflurescence and retinal flat mount showed that A740003 alleviated the retinal edema and neovascularization in ox-LDL injected mice. It indicated that blocking P2 × 7R prevented the inflammatory responses and angiogenesis induced by ox-LDL effectively.

P2 × 7R is an ATP ligand-gated non-selective cation channel that is a member of the purine receptor family [25]. It was verified that P2 × 7R involved in the activation of NLRP3 inflammasome. P2 × 7R activated channel protein pannexin-1, leading to the influx of activating molecules and efflux of K^+ from cell, resulting in NLRP3 inflammasome activation in hepatic stellate cell [26]. We detected the P2 × 7R expression in ARPE-19 cells and mouse retinas and discovered the relationship between P2 × 7R and NLRP3 inflammasome activation. We screened several concentrations of A740003 for treatment in ARPE-19 cells. We found that 1 μM A740003 reduced the expression of NLRP3, Caspase-1 and P2 × 7R significantly in ARPE-19 cells exposed to ox-LDL for 24 hours. However, 200 μM A740003 was required to inhibit the expression of HIF-1α and VEGF increased with ox-LDL incubation for 48 hours. It suggested that it would more and more difficult to reverse the harmful effects induced by ox-LDL with development. The underlying mechanisms of this phenomenon need further investigation. We also found that A740003 pretreatment reduced the up-regulated protein level of P2 × 7R induced by ox-LDL. Ox-LDL exposure increased P2 × 7R expression significantly in ARPE-19 cells. However, the protein level of P2 × 7R decreased remarkably in A740003 pretreated cells. Similar regulatory effects of P2 × 7R antagonist on P2 × 7R expression were reported by Jiang et al. and Wu et al. [26, 27]..

Blocking of P2 × 7R reduced ROS overproduction and rescued retinal function

We found that oxidized low density lipoprotein could induce ROS generation in ARPE-19 cells. ROS is an important trigger for cell pyroptosis. ROS could activate NLRP3 inflammasome and induce inflammation [14]. However, A740003 treatment inhibited the ROS production induced by ox-LDL significantly. It manifested that blocking P2 × 7R reduced the ROS overproduction. The underlying mechanisms of decrease in ROS production remains unknown. Besides, ERG resutls showed that ox-LDL induced the retinal function impairment in mouse model. However, daily treatment of A740003 could preserve the retinal function obviously in mouse injected with ox-LDL.It showed that blocking P2 × 7R could rescue the retinal function to some extent.

The protect effects was associated with the NLRP3 inflammasome and the NF-κB signaling pathway

The results showed that blocking P2 × 7R could decrease the protein levels of NLRP3, Capase-1, IL-1β and P2 × 7R significantly both in ARPE-19 cells and mice. It revealed that A740003 suppressed the activation of NLRP3 inflammasome and alleviated the inflammation induced by ox-LDL. Moreover, we found that blocking P2 × 7R inhibited the phosphorylation of IKBα induced by ox-LDL significantly both in cells and mouse retinas. It indicated that A740003 could inhibit the activation of NF-κB pathway effectively. Besides, we also found that the subretinal injection of ox-LDL induced retinal edema in mice and A740003 alleviated the retinal edema to some extent.

We verified that a single subretinal injection of ox-LDL induced the activation of NLRP3 inflammasome and NF-κB signaling pathway in mice. Once NLRP3 inflammasome was activated, it would recruit ASC and mediate the auto-activation of pro-Caspase-1. The assembled NLRP3 inflammasome then turned itself into a cytokine processing platform by cleaving pro-IL1β/pro-IL-18 into mature peptides and releasing them into extracellular space for downstream inflammatory effects [14]. In brief, ox-LDL produced a large amount of ROS and thus activated NLRP3 inflammasome, and then promoted the secretion of inflammatory cytokines including IL-1β and IL-18. IL-1β and IL-18 are major inflammatory factors found in drusen of AMD patients [28]. We found ox-LDL subretinal injection could promote the secretion of IL-1β significantly in mice. We also found that the subretinal injection of ox-LDL induced retinal edema.

Moreover, ROS generation induced by ox-LDL can also lead the activation of NF-κB signaling pathway. NF-κB signaling pathway is also involved with inflammation response. NF-κB is a nuclear transcription factor that regulates expression of a large number of genes that are critical for the regulation of apoptosis and inflammation. The activation of NF-κB signaling pathway could promote the transcription of NLRP3. The various stimuli that activate NF-κB would cause phosphorylation of IκB, which is followed by its ubiquitination and subsequent degradation [14].

The results indicated that ox-LDL induced retinal inflammation and neovascularization through activation of NF-κB pathway and NLRP3 inflammasome, induction of ROS generation, and up-regulating the expression of HIF-1α and VEGF.

Although the study reveals strong evidence for the pathogenic roles of ox-LDL and therapeutic effects of A740003 in AMD, there are still some limitations that must be addressed. First, the direct interaction of P2 × 7R and NLRP3 needs further investigation, which may provide more details about the relationship between the activation of P2 × 7R and NLRP3 inflammasome. Moreover, further researches and trails need to be performed to testify the effectiveness and safety of P2 × 7R antagonist. There is still a long way to go before applying the P2 × 7R antagonist to AMD in clinic.

Conclusions

In conclusion, we demonstrated that A740003 significantly reduced inflammatory responses and angiogenic factors in ARPE-19 cells induced by ox-LDL. In addition, the intraperitoneal injection of A740003 prevented retinal inflammation and neovascularization, and preserved retinal function in C57BL/6 mice subretinally injected with ox-LDL. The P2 × 7R antagonist could reduce retinal inflammation, neovascularization, and protect retinal function by regulating NLRP3 inflammasome and NF-κB pathway, suppression of ROS generation, as well as inhibition of HIF-1α and VEGF. The results provide a new clue for therapeutic strategies to treat retinal inflammation and neovascularization.

Abbreviations

AMD
Age-related macular degeneration; AOD:Average optical density; ARVO:Association for Research in Vision and Ophthalmology; ASC:Apoptosis-associated speck-like protein containing a caspase recruitment domain; ATP:Adenosine triphosphate; BCA:Bicinchoninic acid; DMSO:Dimethyl sulfoxide; ERG:Electroretinogram; HIF-1α:Hypoxia-inducible factor 1-alpha; IKBα:Inhibitor of nuclear factor-κB alpha; IL-18:Interleukin-18; IL-1β:Interleukin-1 beta; INL:Inner nuclear layer; LDL:Low density lipoprotein; NF-κB:Nuclear factor-κB; NLR:Nod-like receptor; NLRP3:Nod-like receptor pyrin-domain protein 3; ONL:Outer nuclear layer; ox-LDL:oxidized low density lipoprotein; pIKBα:Phosphorylated IKBα; PVDF:Polyvinylidene difluoride; P2 × 7R:P2 × 7 receptor; ROS:Reactive oxygen species; RPE:Retinal pigmented epithelial; SEM:Standard error of mean; TNF-α:Tumor necrosis factor-alpha; VEGF:Vascular endothelial growth factor

Declarations

Availability of data and materials

All data generated or analysed during this study are included in this published article and its supplementary information files.

Ethics approval and consent to participate

The use of animals in these experiments was in accordance with the guidelines established by the Ethics Committee of Henan Eye Institute.

Consent for publication

Not applicable.

Competing interests

The authors declare that they have no competing interests.

Funding

This work was supported by Key Technologies Research and Development Program of Henan Science and Technology Bureau (192102310076), and Henan Health Commission (LHGJ20190820, SBGJ2018081) and National Natural Science Foundation of China grants (81770949).

Authors’ contributions

BL and MZY designed the study and wrote the manuscript. MZY performed the in vivo and in vitro experiments, gathered and analyzed the data. RQQ, WPW and QZ supported the in vitro experiments. JYL and YL supported the in vivo experiments. All authors read and approved the final manuscript.

Acknowledgements

We would like to thank Professor Jikui Shen from John Hopkins University for his inspiration and help.

References

1. van Lookeren Campagne M, LeCouter J, Yaspan BL, Ye W. Mechanisms of age-related macular degeneration and therapeutic opportunities. J Pathol. 2014;232(2):151–64.
2. Cherepanoff S, McMenamin P, Gillies MC, Kettle E, Sarks SH. Bruch's membrane and choroidal macrophages in early and advanced age-related macular degeneration. Br J Ophthalmol. 2010;94(7):918–25.
3. Gehrs KM, Jackson JR, Brown EN, Allikmets R, Hageman GS. Complement, age-related macular degeneration and a vision of the future. Arch Ophthalmol. 2010;128(3):349–58.
4. Wong CW, Yanagi Y, Lee WK, Ogura Y, Yeo I, Wong TY, et al. Age-related macular degeneration and polypoidal choroidal vasculopathy in Asians. Prog Retin Eye Res. 2016;53:107–39.
5. Nowak M, Swietochowska E, Marek B, Szapska B, Wielkoszynski T, Kos-Kudla B, et al. Changes in lipid metabolism in women with age-related macular degeneration. Clin Exp Med. 2005;4(4):183–7.
6. Capra S, Bauer J, Davidson W, Ash S. Nutritional therapy for cancer-induced weight loss. Nutr Clin Pract. 2002;17(4):210–3.
7. Helin-Toiviainen M, Ronkko S, Kaarniranta K, Puustjarvi T, Rekonen P, Ollikainen M, et al. Oxidized low-density lipoprotein, lipid and calcium aggregates reveal oxidative stress and inflammation in the conjunctiva of glaucoma patients. Acta ophthalmologica. 2017;95(4):378–85.
8. Hoppe G, Marmorstein AD, Pennock EA, Hoff HF. Oxidized low density lipoprotein-induced inhibition of processing of photoreceptor outer segments by RPE. Invest Ophthalmol Vis Sci. 2001;42(11):2714–20.
9. Gordiyenko N, Campos M, Lee JW, Fariss RN, Sztein J, Rodriguez IR. RPE cells internalize low-density lipoprotein (LDL) and oxidized LDL(oxLDL) in large quantities in vitro and in vivo. Invest Ophthalmol Vis Sci. 2004;45(8):2822–9.
10. Yamada Y, Tian J, Yang Y, Cutler RG, Wu T, Telljohann RS, et al. Oxidized low density lipoproteins induce a pathologic response by retinal pigmented epithelial cells. Journal of neurochemistry. 2008;105(4):1187–97.
11. Kamei M, Yoneda K, Kume N, Suzuki M, Itabe H, Matsuda K, et al. Scavenger receptors for oxidized lipoprotein in age-related macular degeneration. Invest Ophthalmol Vis Sci. 2007;48(4):1801–7.

12. Javadzadeh A, Ghorbanihaghjo A, Bahreini E, Rashtchizadeh N, Argani H, Alizadeh S. Serum paraoxonase phenotype distribution in exudative age-related macular degeneration and its relationship to homocysteine and oxidized low-density lipoprotein. Retina. 2012;32(4):658–66.
13. Zhang SX, Wang JJ, Dashti A, Wilson K, Zou MH, Szweda L, et al. Pigment epithelium-derived factor mitigates inflammation and oxidative stress in retinal pericytes exposed to oxidized low-density lipoprotein. J Mol Endocrinol. 2008;41(3):135–43.
14. Gao J, Liu RT, Cao S, Cui JZ, Wang A, To E, et al. NLRP3 inflammasome: activation and regulation in age-related macular degeneration. Mediators Inflamm. 2015;2015:690243.
15. Bergsbaken T, Fink SL, Cookson BT. Pyroptosis: host cell death and inflammation. Nat Rev Microbiol. 2009;7(2):99–109.
16. Celkova L, Doyle SL, Campbell M. NLRP3 inflammasome and pathobiology in AMD. J Clin Med. 2015;4(1):172–92.
17. Khalafalla MG, Woods LT, Camden JM, Khan AA, Limesand KH, Petris MJ, et al. P2 × 7 receptor antagonism prevents IL-1beta release from salivary epithelial cells and reduces inflammation in a mouse model of autoimmune exocrinopathy. The J Biol Chem. 2017;292(40):16626–37.
18. Dong L, Hu Y, Zhou L, Cheng X. P2 × 7 receptor antagonist protects retinal ganglion cells by inhibiting microglial activation in a rat chronic ocular hypertension model. Mol Med Rep. 2017;17(2):2289–96.
19. Hu H, Yang B, Li Y, Zhang S, Li Z. Blocking of the P2 × 7 receptor inhibits the activation of the MMP-13 and NF-kB pathways in the cartilage tissue of rats with osteoarthritis. Int J Mol Med. 2016;38(6):1922–32.
20. Mao K, Shu W, Liu L, Gu Q, Qiu Q, Wu X. Salvianolic acid A inhibits ox-LDL effects on exacerbating choroidal neovascularization via downregulating CYLD. Oxid Med Cell Longev. 2017;2017:6210694.
21. Qiu Y, Tao L, Zheng S, Lin R, Fu X, Chen Z, et al. AAV8-mediated angiotensin-converting enzyme 2 gene delivery prevents experimental autoimmune uveitis by regulating MAPK, NF-kB and STAT3 pathways. Sci Rep. 2016;6:31912.
22. Zheng S, Yang H, Chen Z, Zheng C, Lei C, Lei B. Activation of liver X receptor protects inner retinal damage induced by N-methyl-D-aspartate. Invest Ophthalmol Vis Sci. 2015;56(2):1168–80.
23. Mori K, Duh E, Gehlbach P, Ando A, Takahashi K, Pearlman J, et al. Pigment epithelium-derived factor inhibits retinal and choroidal neovascularization. J Cell Physiol. 2001;188(2):253–63.
24. Wang Y, Wang M, Zhang X, Zhang Q, Nie J, Zhang M, et al. The association between the lipids levels in blood and risk of age-related macular degeneration. Nutrients. 2016;8(10).
25. Gu BJ, Saunders BM, Petrou S, Wiley JS. P2 × (7) is a scavenger receptor for apoptotic cells in the absence of its ligand, extracellular ATP. J Immunol. 2011;187(5):2365–75.
26. Jiang S, Zhang Y, Zheng JH, Li X, Yao YL, Wu YL, et al. Potentiation of hepatic stellate cell activation by extracellular ATP is dependent on P2 × 7R-mediated NLRP3 inflammasome activation. Pharmacol Res. 2016;117:82–93.

27. Wu X, Ren J, Chen G, Wu L, Song X, Li G, et al. Systemic blockade of P2 × 7 receptor protects against sepsis-induced intestinal barrier disruption. Sci Rep. 2017;7(1):4364.
28. Marneros AG. NLRP3 inflammasome blockade inhibits VEGF-A-induced age-related macular degeneration. Cell Rep. 2013;4(5):945–58.

Figures

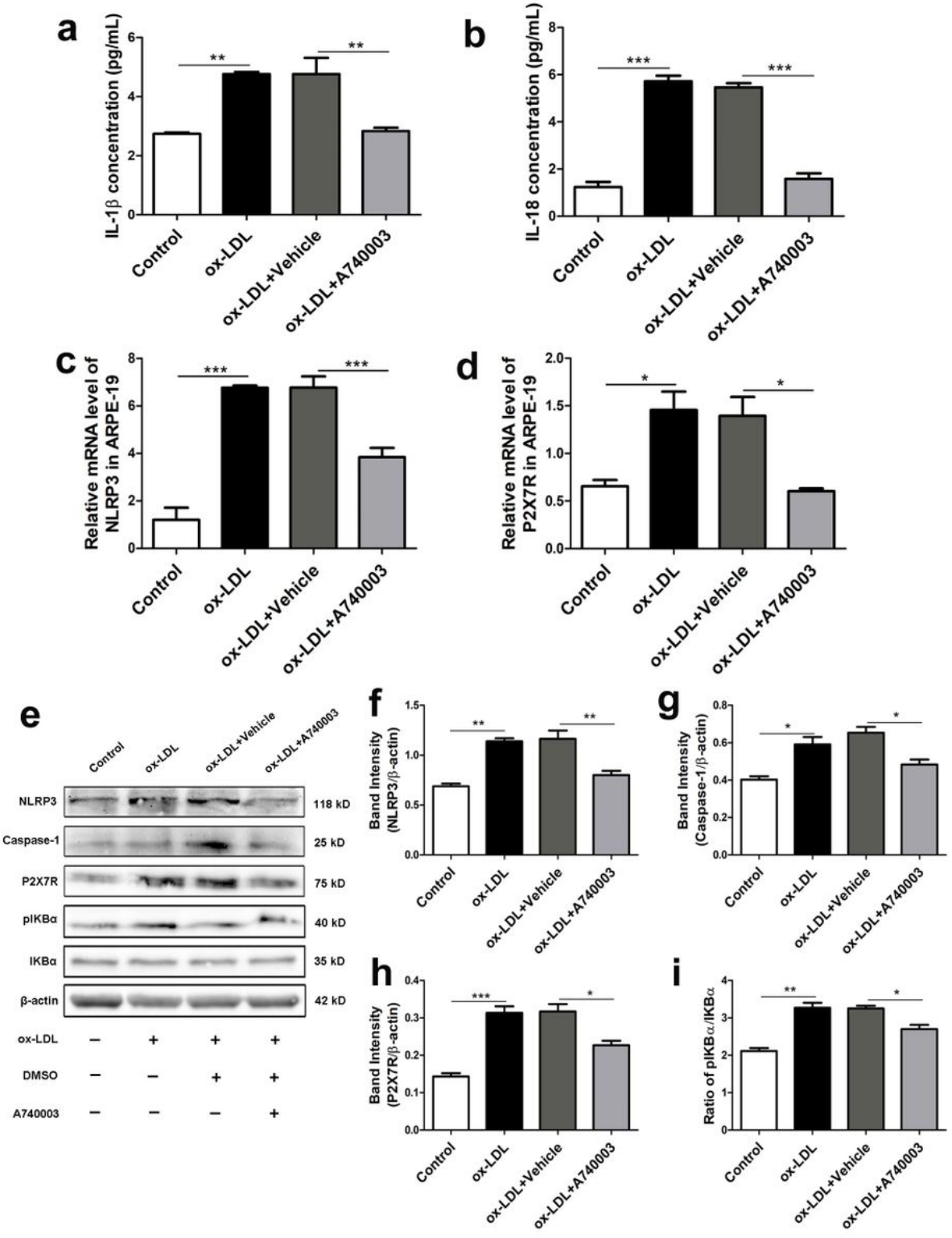

Figure 1

A740003 inhibited the activation of NLRP3 inflammasome, phosphorylation of IKB and decreased the expression of P2X7R in ARPE-19 cells exposed to ox-LDL for 24 hours. ELISA results showed that A740003 pretreatment decreased the secretion of inflammatory cytokines including IL-1 (a) and IL-18 (b) significantly compared to vehicle-treated group. Besides, the mRNA levels of NLRP3 and P2X7R were detected by qPCR. A740003 pretreatment inhibited the increase of NLRP3 (c) and P2X7R (d) at mRNA level significantly in ARPE-19 cells. A740003 inhibited the over expression of P2X7R and NLRP3 which were induced by ox-LDL. Western Blot showed that ox-LDL increased the protein levels of NLRP3 (e, f), Caspase-1 (e, g), P2X7R e, h and induced the phosphorylation of IKB e, i significantly, While A740003 inhibited the up-regulation of NLRP3, Caspase-1, P2X7R and the phosphorylation of IKB significantly. The results were mean ± SEM. Significance of difference (*p<0.05, **p<0.01, ***p<0.001) was determined by using one-way ANOVA with Bonferroni correction.

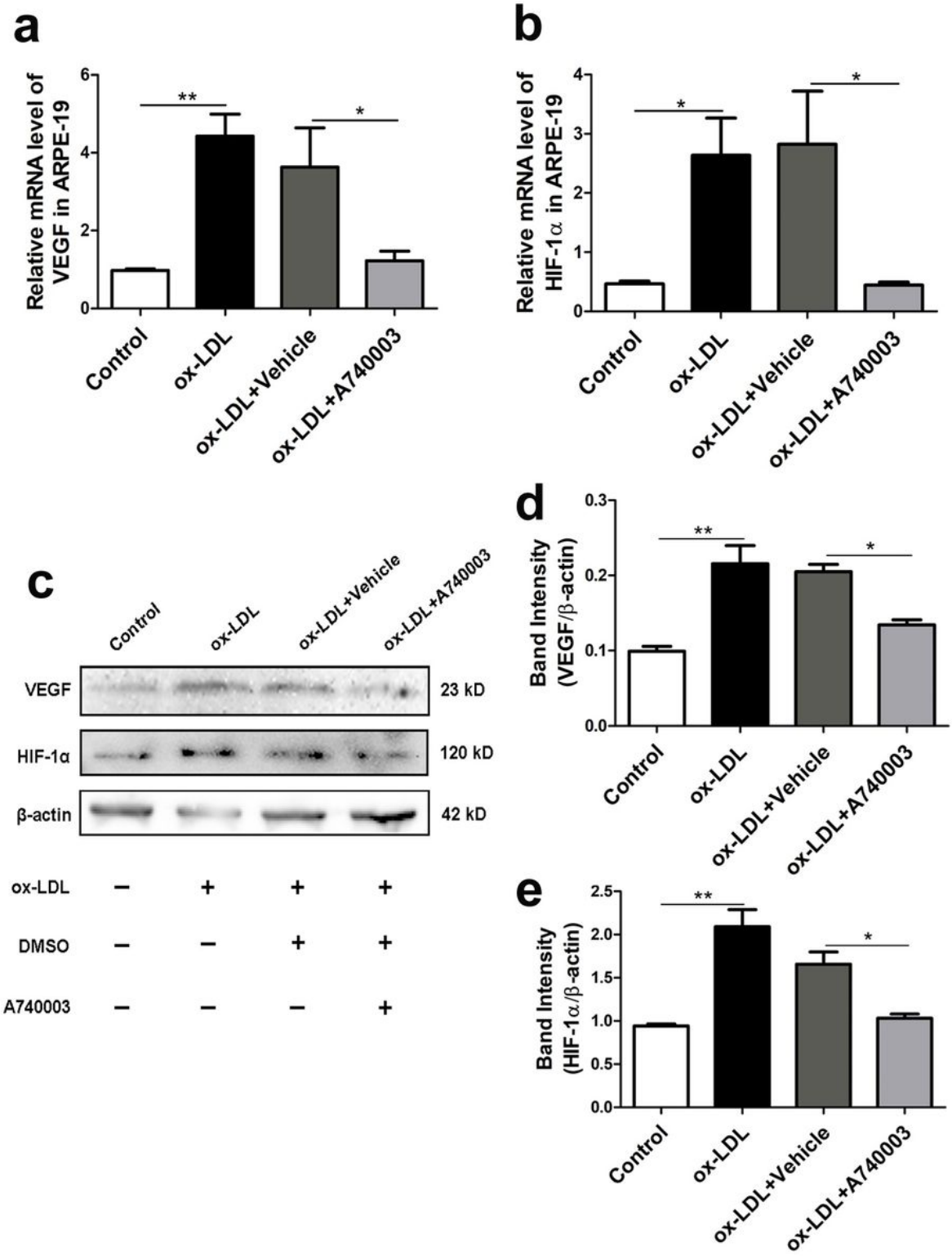

Figure 2

A740003 suppressed the up-regulation of angiogenic growth factors in ARPE-19 cells induced by ox-LDL incubation for 48 hours. The mRNA levels of VEGF and HIF-1□□were detected by qPCR. Compared to vehicle-treated group, A740003 pretreatment significantly suppressed the increase of VEGF □a□ and HIF-1□□□b□□in ARPE-19 cells induced by ox-LDL□ Besides, the protein levles of VEGF and HIF-1□□were detected by Western Blot. A740003 pretreatment also decreased the over expression of VEGF (c, d) and HIF-1□□□c,

e induced by ox-LDL. The results were mean ± SEM. Significance of difference (*p<0.05, **p<0.01, ***p<0.001) was determined by using one-way ANOVA with Bonferroni correction.

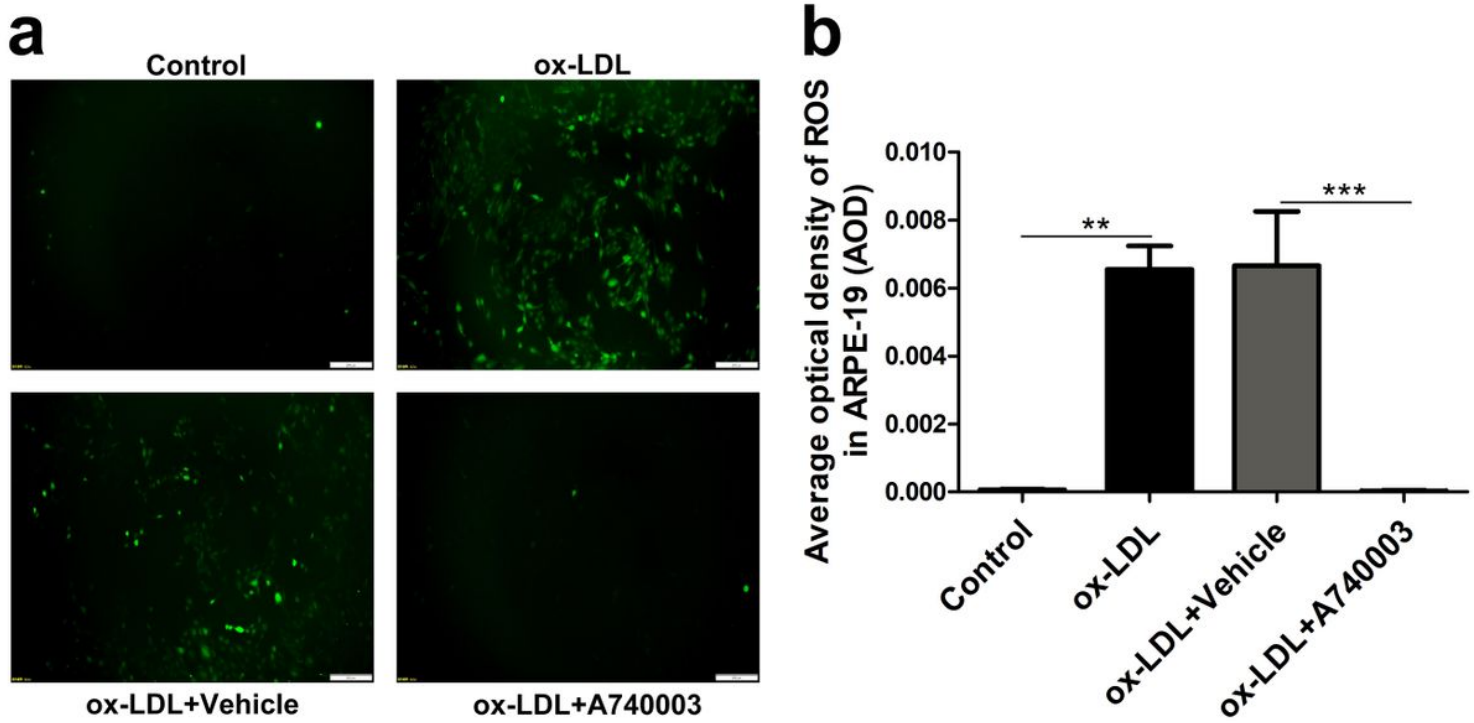

Figure 3

A740003 inhibited the ROS production in ARPE-19 cells induced by ox-LDL. The fluorescence of DCFH-DA increased robustly in ARPE-19 cells incubated with ox-LDL (a). The average optical density of ROS in ox-LDL group was obviously higher than control group (b). However, A740003 pretreatment could decrease the fluorescence of DCFH-DA in ARPE-19 cells induced by ox-LDL (a, b). The over production of ROS induced by ox-LDL were suppressed by A740003. The results were mean ± SEM. Significance of difference (*p<0.05, **p<0.01, ***p<0.001) was determined by using one-way ANOVA with Bonferroni correction.

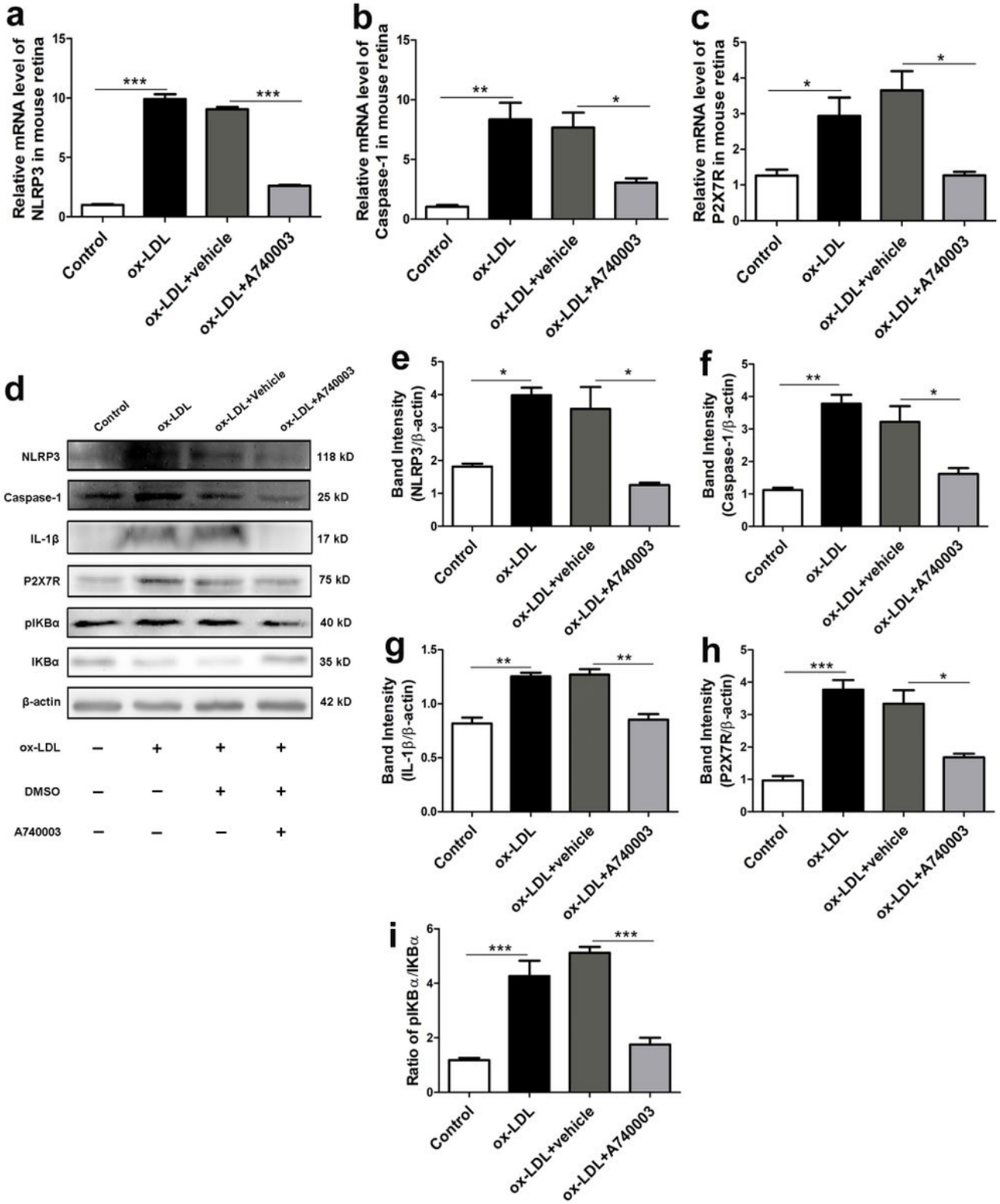

Figure 4

A740003 inhibited the activation of NLRP3 inflammasome, phosphorylation of IKB and decreased the over expression of P2X7R in C57BL/6 mouse retinas injected with ox-LDL. The qPCR showed that mRNA levels of NLRP3 (a), Caspase-1 (b) and P2X7R (c) in C57BL/6 mouse retina increased significantly 14 days after subretinal injection of ox-LDL. Compared to vehicle-treated group, intraperitoneally injection of A740003 reduced mRNA expression of NLRP3 (a), Caspase-1 (b) and P2X7R (c) obviously. Moreover,

Western Blot showed that protein levels of NLRP3 (d, e), Caspase-1 (d, f), IL-1β (d, g) and P2X7R (d, h) in C57BL/6 mouse retina were up-regulated after subretinal injection of ox-LDL, while which were inhibited by A740003 significantly. The phosphorylation of IKBα (d, i) in C57BL/6 mouse retina was also promoted by ox-LDL, and A740003 treatment could decreased the phosphorylation of IKBα induced by ox-LDL. The results were mean ± SEM. Significance of difference (*p<0.05, **p<0.01, ***p<0.001) was determined by using one-way ANOVA with Bonferroni correction. (n=4-6)

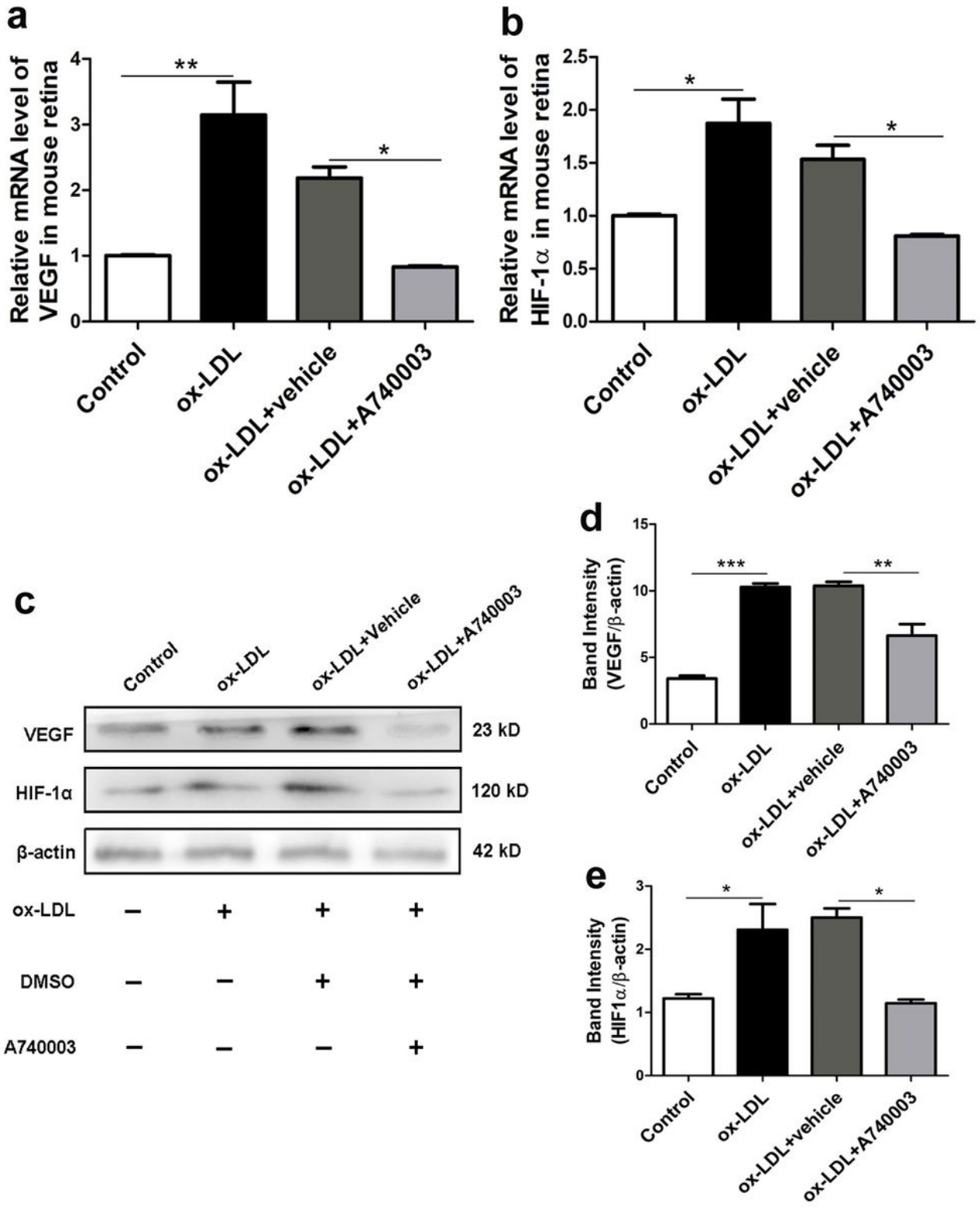

Figure 5

A740003 inhibited the up-regulation of VEGF and HIF-1□□in C57BL/6 mouse retinas injected with ox-LDL. The mRNA levels of VEGF and HIF-1□□were detected by qPCR. Compared to vehicle-treated group, intraperitoneally injection of A740003 significantly inhibited the increase of VEGF □a□ and HIF-1□□□b□□in C57BL/6 mouse retina induced by ox-LDL□□Western Blot showed that protein levels of VEGF (c, d) and HIF-1□ (c, e) in C57BL/6 mouse retina were up-regulated by subretinal injection of ox-LDL, while which were suppressed by A740003 significantly. The results were mean ± SEM. Significance of difference (*p<0.05, **p<0.01, ***p<0.001) was determined by using one-way ANOVA with Bonferroni correction. (n=4-6)

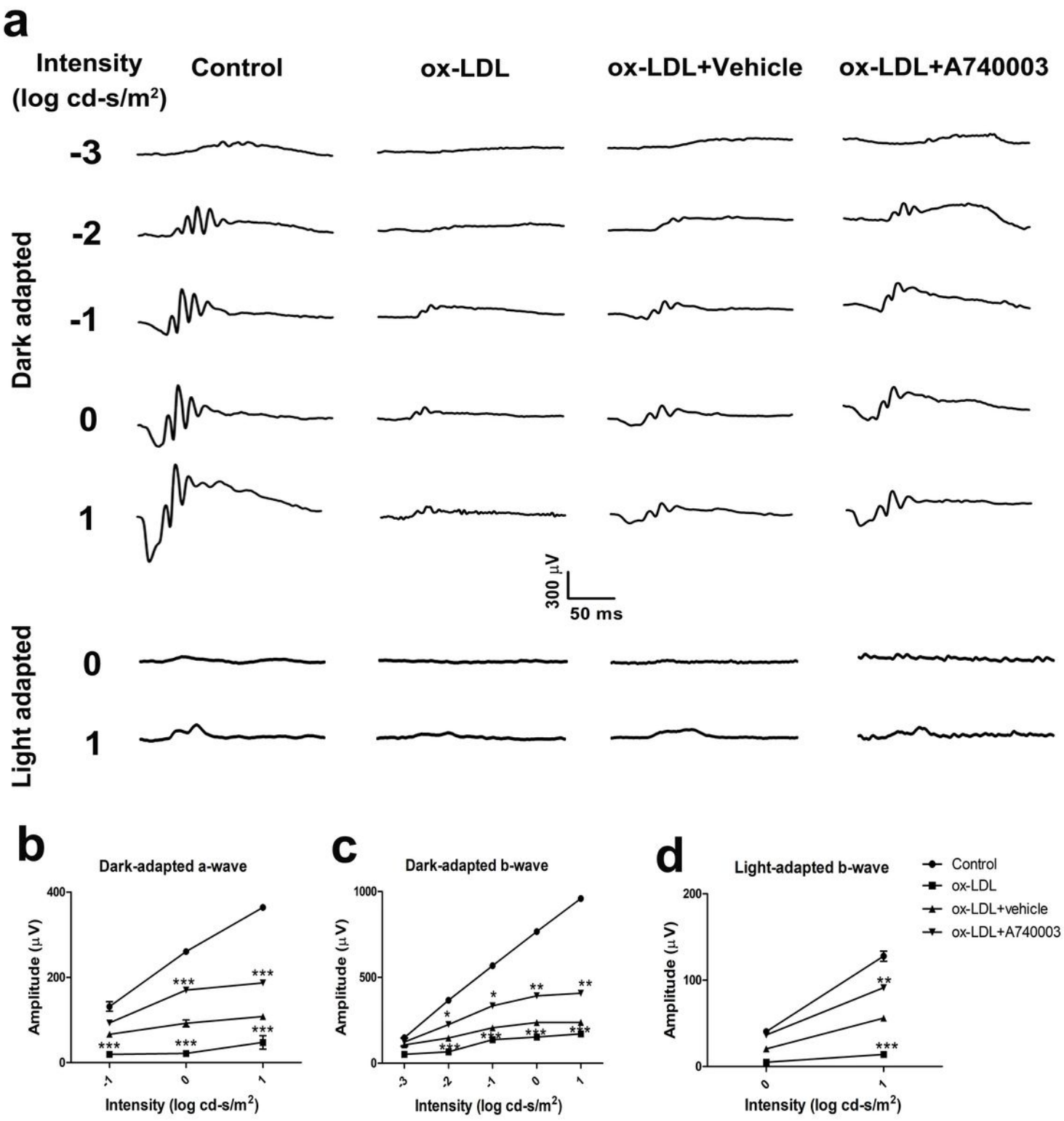

Figure 6

Retinal functions of C57BL/6 mice were assessed by dark- and light-adapted ERG. A740003 prevented the malfunction in C57BL/6 mouse retinas induced by ox-LDL. ERG was performed at 14 days after subretinal injection of ox-LDL. Representative ERG responses in the control, the ox-LDL, the ox-LDL plus vehicle-treated, and the ox-LDL plus A740003-treated groups (a) were shown. The ERG amplitudes vs. Flash intensity profiles for the dark-adapted a-wave (b), dark-adapted b-wave (c), and the light-adapted b-

wave (d) were summarized. Intraperitoneally injection of A740003 significantly preserved the ERG amplitudes compared to vehicle-treated group. The results were mean ± SEM. Significance of difference (*p<0.05, **p<0.01, ***p<0.001) was determined by using two-way ANOVA with Bonferroni correction. (n=6-8)

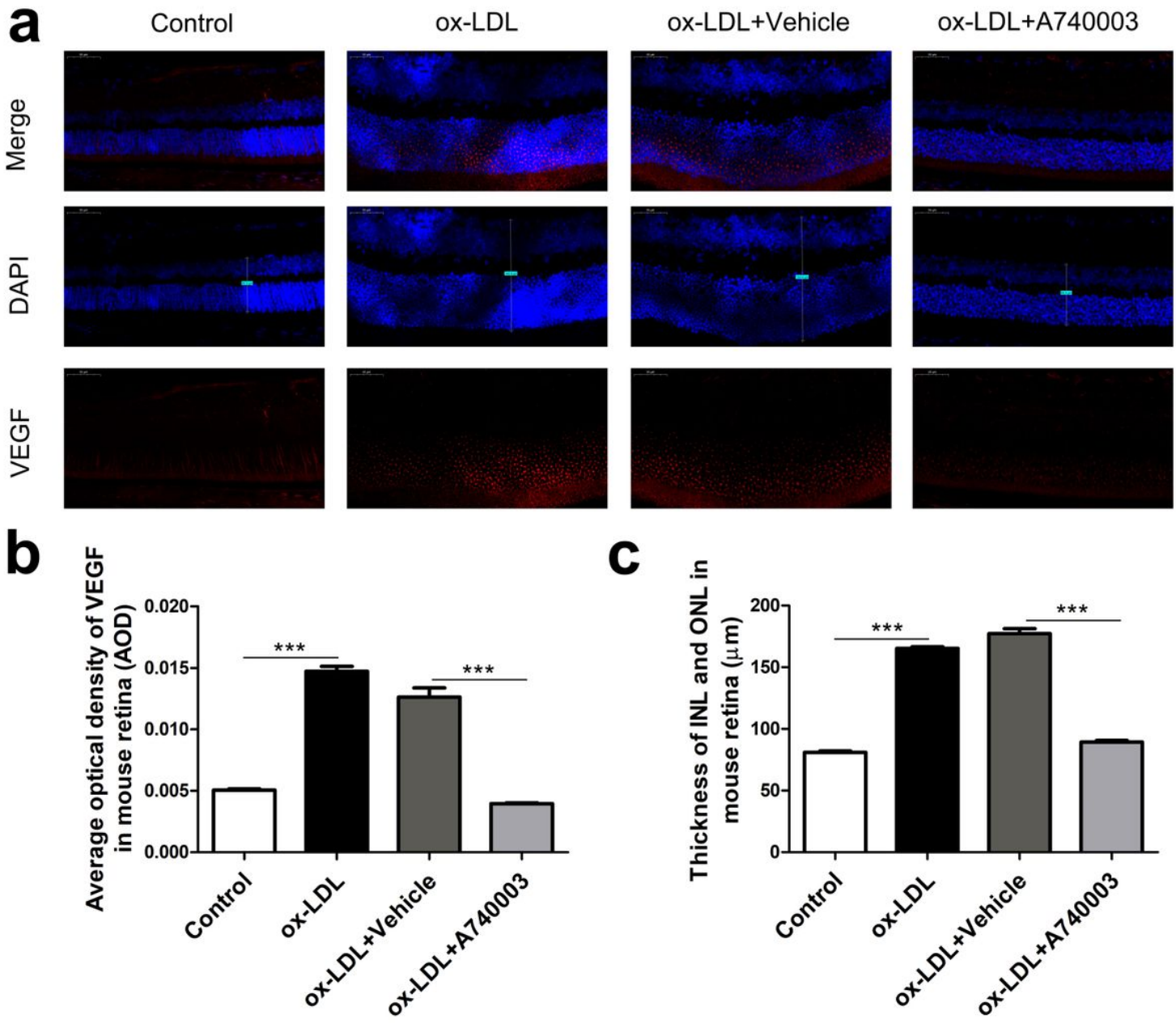

Figure 7

Protective effects of A740003 on the retinal angiogenesis and edema of C57BL/6 mice induced by ox-LDL. The retinal angiogenesis and edema in C57BL/6 mice were assessed by immunofluorescent staining of paraffin sections of whole eyes (a). Nuclei of cells in INL and ONL were stained by DAPI (blue; a) and VEGF was indicated by secondary antibody (red; a). The average optical density of VEGF (b) and the thickness of INL and ONL (c) in mouse retina were summarized. Compared to vehicle-treated group, A740003 decreased the VEGF expression and retinal edema significantly in mouse retina induced by ox-

LDL. Scale bar: 50 □m. Abbreviations: INL: inner nuclear layer; ONL: outer nuclear layer. The results were mean ± SEM. Significance of difference (*p<0.05, **p<0.01, ***p<0.001) was determined by using one-way ANOVA with Bonferroni correction. (n=4-6)

Supplementary Files

This is a list of supplementary files associated with this preprint. Click to download.

- Flg.S1.tif
- Flg.S1.tif
- Flg.S1.tif
- SupplementaryMaterial.doc
- SupplementaryMaterial.doc
- SupplementaryMaterial.doc